VIP Coordination Chemistry

DOI: 10.1002/ange.201107880

Observation of the Highest Coordination Number in Planar Species: Decacoordinated Ta©B_{10}^- and Nb©B_{10}^- Anions**

Timur R. Galeev, Constantin Romanescu, Wei-Li Li, Lai-Sheng Wang, and Alexander I. Boldyrev**

Coordination number is one of the most fundamental characteristics of molecular structures. Molecules with high coordination numbers often violate the octet and the 18 electron rules and push the boundary of our understanding of chemical bonding and structures. We have been searching for the highest possible coordination number in a planar species with equal distances between the central atom and all peripheral atoms. To successfully design planar chemical species with such high coordination one must take into account both mechanical and electronic factors. The mechanical factor requires the right size of the central atom to fit into the cavity of a monocyclic ring. The electronic factor requires the right number of valence electrons to achieve electronic stability of the high-symmetry structure. Boron is known to form highly symmetric planar structures owing to its ability to participate simultaneously in localized and delocalized bonding.[1–7] The planar boron clusters consist of a peripheral ring featuring strong two-center-two-electron (2c-2e) B–B σ bonds and one or more central atoms bonded to the outer ring through delocalized σ and π bonds. The starting point for the present work is that the bare eight-atom and nine-atom planar boron clusters were found to reach coordination number seven in the D_{7h} B_8 neutral or B_8^{2-} as a part of the LiB_8^- cluster[1,3] or eight in the D_{8h} B_9^- molecular wheel.[1]

The CB_6^{2-}, C_3B_4, and CB_7^- wheel-type structures with hexa- and heptacoordinated carbon atom were first considered computationally by Schleyer and co-workers.[8,9] The high symmetry hypercoordinated structures were found to be local minima because they "fulfill both the electronic and geometrical requirements for good bonding".[8,9] In particular, Schleyer and co-workers pointed out that the wheel structures are π aromatic with 6 π electrons. In joint photoelectron spectroscopy (PES) and theoretical studies it was shown that carbon occupies the peripheral position in such clusters rather than the center, because C is more electronegative than B and thus prefers to participate in localized 2c-2e σ bonding, which is possible only at the circumference of the wheel structures.[10,11] A series of planar wheel-type boron rings with a main group atom in the center and coordination numbers 6–10 have been probed theoretically.[12–14] So far the joint PES and ab initio studies of aluminum-doped boron clusters showed that the aluminum atom avoids the central position in the AlB_6^-, AlB_7^-, AlB_8^-, AlB_9^-, AlB_{10}^-, and AlB_{11}^- systems.[15–17]

Recently, a transition-metal-doped boron cluster, Ru©B_9^-, with the highest coordination number known to date was reported.[18] We developed a chemical bonding model, which allows the design of planar molecules with high coordination numbers.[18] According to the model, $2n$ electrons in the M©B_n species form n 2c-2e peripheral B–B σ bonds. The remaining valence electrons form two types of delocalized bonding, in-plane σ and out-of-plane π bonding, and therefore, should satisfy the $(4N+2)$ Hückel rule separately for σ and π aromaticity to attain highly symmetric structures with high electronic stability. In pure wheel-type boron clusters each B atom in the circumference contributes two electrons to the B–B peripheral covalent bonds and one electron to the delocalized bonds, whereas the central B atom contributes all its valence electrons to the delocalized bonds. Thus, out of 26 valence electrons in B_8^{2-} or 28 in B_9^-, 14 or 16 valence electrons form peripheral covalent 2c-2e σ bonds, leaving six σ and six π electrons ($N=1$ for the $4N+2$ rule) for double (σ and π) aromaticity. However, pure planar boron clusters cannot go beyond coordination number eight because of the mechanical factor (the small size of the central boron atom). For example, the B_{10} cluster does not contain a nine-coordinated boron atom, because the boron atom is too small to fit in the central position of a B_9 ring.[2] Since the central atom participates only in delocalized bonding, atoms more electronegative than boron such as carbon avoid the central position.[10,11,19] Transition-metal atoms, on the other hand, are well-suited for the central position in M©B_n species. To satisfy the peripheral B–B bonding and the σ and π Hückel aromaticity for $N=1$, the electronic requirement for the central atom in high-symmetry species, such as M©B_n^{k-}, is $x=12-n-k$, where x is the valence of the transition-metal atom M. Ru©B_9^- satisfies the formula and is the first example of an

[*] T. R. Galeev, Prof. Dr. A. I. Boldyrev
Department of Chemistry and Biochemistry
Utah State University, Logan, UT 84322 (USA)
E-mail: a.i.boldyrev@usu.edu
Homepage: http://www.chem.usu.edu/~boldyrev/
Dr. C. Romanescu, W. L. Li, Prof. Dr. L. S. Wang
Department of Chemistry, Brown University
Providence, RI 02912 (USA)
E-mail: lai-sheng_wang@brown.edu
Homepage: http://www.chem.brown.edu/research/LSWang/

[**] We thank Dr. Boris B. Averkiev for the theoretical calculations of the relativistic spin–orbit splittings in TaB_{10}^- with the ADF software. This work was supported by the National Science Foundation (grant DMR-0904034 to L.S.W. and grant CHE-1057746 to A.I.B.). Computer time from the Center for High Performance Computing at USU and an allocation of computer time from the Center for High Performance Computing at the University of Utah are gratefully acknowledged. T.R.G. thanks Utah State University for the Vice President for Research Graduate Fellowship.

Supporting information for this article is available on the WWW under http://dx.doi.org/10.1002/anie.201107880.

experimentally observed planar species with coordination number nine.[18]

The quest for higher coordination numbers was limited primarily to theoretical calculations.[12,20,21] The highest coordination number considered computationally was ten for a broad range of metal atoms: CB_{10}^{2+}, SiB_{10}^{2+}, GeB_{10}^{2+}, SnB_{10}^{2+}, PbB_{10}^{2+},[12] AuB_{10}^{-}, AgB_{10}^{-}, CdB_{10}, HgB_{10}, InB_{10}^{+}, TlB_{10}^{+},[20] and ScB_{10}^{3-}, TiB_{10}^{2-}, VB_{10}^{-}, FeB_{10}^{2+}, NiB_{10}^{2+}, CuB_{10}^{3+}, CuB_{10}^{-}, ZnB_{10}.[21] Though some of these proposed species satisfy our electronic design principle, none was known to be the global minimum. Among these species, only AuB_{10}^{-} has been experimentally observed,[22] but its global minimum was shown to be an Au atom interacting with a B_{10}^{-} cluster on the outside: the wheel-type structure is a high-energy isomer, around 45 kcal mol^{-1} above the ground state.[22] The instability of the Au©B_{10}^{-} wheel isomer is caused by the fact that only the 6s valence electron participates in the delocalized bonding in this species while the 5d orbitals of the central Au atom are completely filled and have little interaction with the peripheral B_{10} ring. Our recent finding of the nonacoordinated Ru©B_9^{-} complex shows that the interactions of the 4d orbitals with the B_9 ring play an important role in stabilizing the wheel structure. Early 4d and 5d transition metals have larger atomic sizes and more diffused d orbitals, conducive to participation in bonding with the peripheral boron rings. Thus, our search for higher coordination metal-doped boron clusters has been focused on the early 4d or 5d transition metals.

Here we show that Nb and Ta fit into the B_{10} decagonal ring and the resulting singly charged wheel-type anions Nb©B_{10}^{-} and Ta©B_{10}^{-} are closed-shell and doubly aromatic systems. Furthermore, all five valence electrons of Nb and Ta participate in the delocalized bonding, providing considerable stability to the wheel structures, which were found to be the lowest energy isomers by unbiased global minimum searches (alternative structures found for TaB_{10}^{-} and NbB_{10}^{-} are presented in Figures S1 and S2 in the Supporting Information). The theoretical results are in excellent agreement with the experimental photoelectron data, confirming the first decacoordinated 2D chemical species.

The TaB_{10}^{-} and NbB_{10}^{-} clusters were produced in a laser-vaporization supersonic molecular beam cluster source and probed using photoelectron spectroscopy (see the Experimental Section). The photoelectron spectra of TaB_{10}^{-} and NbB_{10}^{-} at two different photon energies are shown in Figure 1. The spectrum of TaB_{10}^{-} at 193 nm (Figure 1 a) shows a fairly simple spectral pattern with three strong peaks (X, A, B) between 3.9–4.7 eV and two weak bands (C, D) between 5.2–5.6 eV. At 266 nm (Figure 1 b), an additional peak was resolved between the X and A band. This peak is due to a vibrational feature of the X band, yielding a vibrational spacing of (1050 ± 50) cm^{-1}. The first adiabatic detachment energy (ADE) and the vertical detachment energy (VDE) for TaB_{10}^{-}, both defined by the 0–0 transition of the X band, are (4.04 ± 0.03) eV, which also represents the electron affinity of neutral Ta©B_{10}. The spectra of NbB_{10}^{-} (Figure 1 c and 1 d) are very similar to those of TaB_{10}^{-} except for the weak low binding energy features labeled as X′, A′, B′, and C′. This observation suggests the presence of a higher energy

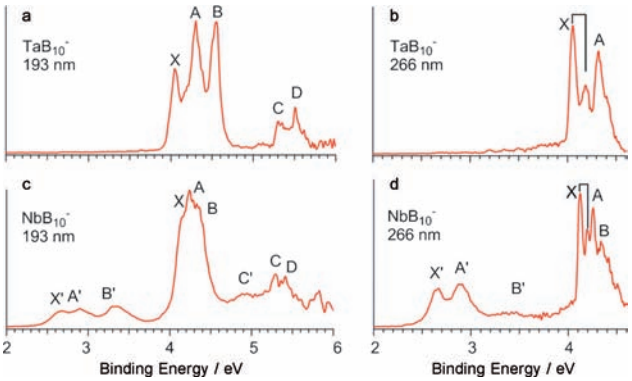

Figure 1. Photoelectron spectra of TaB_{10}^{-} at a) 193 nm and b) 266 nm. Photoelectron spectra of NbB_{10}^{-} at c) 193 nm and d) 266 nm. The vertical lines in (b) and (d) are vibrational structures.

isomer in the beam of NbB_{10}^{-}, whereas the main isomer of NbB_{10}^{-} should be similar to that of TaB_{10}^{-}. The X, A, B features in the NbB_{10}^{-} spectra are more congested and fine features are also resolved at 266 nm (Figure 1 d), yielding a vibrational frequency for the ground state of NbB_{10} as (600 ± 50) cm^{-1}. The vibrationally resolved X band yields an accurate ADE for NbB_{10}^{-} as (4.10 ± 0.03) eV, very close to that for TaB_{10}^{-}. The observed VDEs for all spectral features for TaB_{10}^{-} and NbB_{10}^{-} are given in Table 1, where they are compared with the computational data.

According to the highest level of theory we used, the wheel-type structures (D_{10h}M©B_{10}^{-}) are the global minima for both anions (Figure 2). The second lowest isomers of both species involve the metal atom interacting with the B_{10} cluster from above (C_{2v}). This C_{2v} isomer is close in energy to the global minimum for NbB_{10}^{-} and is likely to be present in the experiment.

To verify the wheel-type structures we computed VDEs for the two lowest isomers of each species (see the Experimental Section). Theoretical VDEs calculated for the M©B_{10}^{-} structures at two non-relativistic levels of theory predict two detachment channels in the 4.0–4.5 eV binding energy range (Table 1), though there are more peaks in the experimental spectra in this region. As shown in Figure S3 in the Supporting Information, both the HOMO (e_{2g}) and HOMO-1 (e_{1u}) of the M©B_{10}^{-} clusters are doubly degenerate involving interactions between the d orbitals and the B_{10} ring. Thus, spin–orbit coupling is expected to yield two photoelectron bands from electron detachment from each orbital, thereby resulting in four detachment bands in this energy region. Hence, the three observed peaks could result from the overlap of the four expected spin–orbit split peaks. Indeed, spin–orbit calculations for Ta©B_{10}^{-} revealed a splitting of around 0.2 eV in these peaks (see Tables S1 and S2 in the Supporting Information), in excellent agreement with the experiment. The calculated VDEs from HOMO-2 and HOMO-3 are also in excellent agreement with the observed bands C and D. We also calculated the vibrational frequencies for the neutral Ta©B_{10} species (see Table S3 in the Supporting Information), the symmetry of which is reduced by the Jahn–Teller effect. The frequency for one of the totally symmetric mode [$\omega_4(a_g) = 1050$ cm^{-1}] is in excellent agreement with the

Table 1: Observed vertical electron detachment energies (VDEs) of TaB_{10}^- and NbB_{10}^- compared with the theoretically calculated values for the two lowest isomers of TaB_{10}^- and NbB_{10}^-. All energies are in eV.

Observed features	VDE (exp)[a]	Final state and electronic configuration	VDE (theoretical)	
			ROPBE1PBE[b]	ROCCSD(T)[c]
$Ta©B_{10}^-$ (D_{10h}, $^1A_{1g}$)				
X[d]	4.04(3)	$^2E_{2g}$ ... $2a_{1g}^2\ 1b_{2u}^2\ 1a_{2u}^2\ 1e_{1g}^4\ 2e_{1u}^4\ 2e_{2g}^3$	4.13	4.16
A	4.29(3)	$^2E_{1u}$ ... $2a_{1g}^2\ 1b_{2u}^2\ 1a_{2u}^2\ 1e_{1g}^4\ 2e_{1u}^3\ 2e_{2g}^4$	4.37	4.46
B[e]	4.55(5)			
C	5.36(5)	$^2E_{1g}$ ... $2a_{1g}^2\ 1b_{2u}^2\ 1a_{2u}^2\ 1e_{1g}^3\ 2e_{1u}^4\ 2e_{2g}^4$	5.37	5.47
D	5.51(5)	$^2A_{2u}$ ... $2a_{1g}^2\ 1b_{2u}^2\ 1a_{2u}^1\ 1e_{1g}^4\ 2e_{1u}^4\ 2e_{2g}^4$	5.49	5.61
TaB_{10}^- (C_{2v}, $^1A_1$)				
		$^2A_1$ ... $5a_1^2\ 4b_2^2\ 4b_1^2\ 3a_2^2\ 6a_1^2\ 7a_1^1$	2.52	2.64
		$^2A_1$ ... $5a_1^2\ 4b_2^2\ 4b_1^2\ 3a_2^2\ 6a_1^1\ 7a_1^2$	2.70	–[f]
		$^2A_2$ ... $5a_1^2\ 4b_2^2\ 4b_1^2\ 3a_2^1\ 6a_1^2\ 7a_1^2$	3.34	3.42
		$^2B_1$ ... $5a_1^2\ 4b_2^2\ 4b_1^1\ 3a_2^2\ 6a_1^2\ 7a_1^2$	4.37	4.43
		$^2B_2$ ... $5a_1^2\ 4b_2^1\ 4b_1^2\ 3a_2^2\ 6a_1^2\ 7a_1^2$	5.00	5.06
$Nb©B_{10}^-$ (D_{10h}, $^1A_{1g}$)				
X[g]	4.12(3)	$^2E_{2g}$ ... $1b_{2u}^2\ 2a_{1g}^2\ 1a_{2u}^2\ 1e_{1g}^4\ 2e_{1u}^4\ 2e_{2g}^3$	4.16	4.21
A	4.26(3)	$^2E_{1u}$ ... $1b_{2u}^2\ 2a_{1g}^2\ 1a_{2u}^2\ 1e_{1g}^4\ 2e_{1u}^3\ 2e_{2g}^4$	4.29	4.36
B[e]	4.34(5)			
C	5.28(5)	$^2E_{1g}$ ... $1b_{2u}^2\ 2a_{1g}^2\ 1a_{2u}^2\ 1e_{1g}^3\ 2e_{1u}^4\ 2e_{2g}^4$	5.32	5.44
D	5.41(5)	$^2A_{2u}$ ... $1b_{2u}^2\ 2a_{1g}^2\ 1a_{2u}^1\ 1e_{1g}^4\ 2e_{1u}^4\ 2e_{2g}^4$	5.42	5.50
NbB_{10}^- (C_{2v}, $^1A_1$)				
X′	2.65(4)	$^2A_1$ ... $5a_1^2\ 4b_2^2\ 4b_1^2\ 3a_2^2\ 6a_1^2\ 7a_1^1$	2.48	2.57
A′	2.89(4)	$^2A_1$ ... $5a_1^2\ 4b_2^2\ 4b_1^2\ 3a_2^2\ 6a_1^1\ 7a_1^2$	2.69	2.84
B′	3.4(1)	$^2A_2$ ... $5a_1^2\ 4b_2^2\ 4b_1^2\ 3a_2^1\ 6a_1^2\ 7a_1^2$	3.23	3.30
		$^2B_1$ ... $5a_1^2\ 4b_2^2\ 4b_1^1\ 3a_2^2\ 6a_1^2\ 7a_1^2$	4.33	4.37
C′	4.91(5)	$^2B_2$ ... $5a_1^2\ 4b_2^1\ 4b_1^2\ 3a_2^2\ 6a_1^2\ 7a_1^2$	4.95	4.99

[a] Numbers in parentheses are the uncertainty in the last digit. [b] The VDEs were calculated at ROPBE0/Ta,Nb/Stuttgart/B/aug-cc-pVTZ. [c] The VDEs were calculated at ROCCSD(T)/Ta,Nb/Stuttgart/B/aug-cc-pVTZ//PBE0/Ta,Nb/Stuttgart/B/aug-cc-pVTZ. [d] Measured ADE = 4.04(3) eV. Calculated ADE at ROCCSD(T)/Ta/Stuttgart/B/aug-cc-pVTZ//PBE0/Ta/Stuttgart/B/aug-cc-pVTZ with ZPE correction: 4.05 eV. [e] The peak is assigned to the transition to the second spin–orbit component of the $^2E_{1u}$ electronic state. [f] We were not able to calculate this VDE at this level of theory. [g] Measured ADE = 4.10(3) eV. Calculated ADE at ROCCSD(T)/Nb/Stuttgart/B/aug-cc-pVTZ//PBE0/Nb/Stuttgart/B/aug-cc-pVTZ with ZPE correction: 4.03 eV.

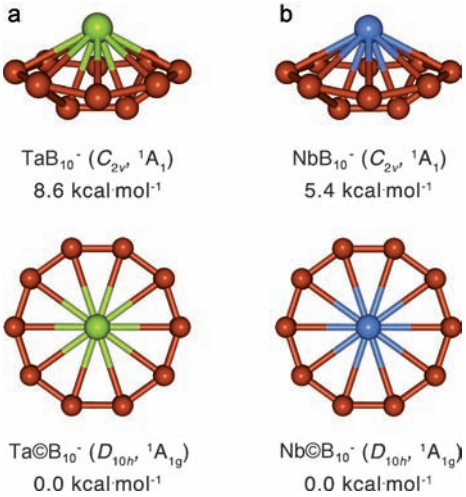

Figure 2. Structures of the two lowest energy isomers of a) TaB_{10}^- and b) NbB_{10}^-, and the their point group symmetries, spectroscopic states, and zero-point energy (ZPE) corrected relative energies (RCCSD(T)/Ta, Nb/Stuttgart/B/aug-cc-pVTZ//PBE0/Ta, Nb/Stuttgart/B/aug-cc-pVTZ).

observed vibrational frequency for the X band. On the other hand, the predicted VDEs for the higher energy C_{2v} isomer of TaB_{10}^- totally disagree with the experimental spectra. Overall, the theoretical results for the D_{10h} $Ta©B_{10}^-$ structure are in excellent agreement with the experimental data, confirming unequivocally that the molecular wheel is the global minimum for TaB_{10}^-. The VDEs calculated for the D_{10h} structure of $Nb©B_{10}^-$ can explain the high energy features (Table 1, X, A–D), which are similar to those of the features in the $Ta©B_{10}^-$ spectra. The smaller spin–orbit effects expected in $Nb©B_{10}^-$ result in the more congested spectral features in the 4.0–5.4 eV energy range (Figure 1c and 1d). The additional features (X′, A′, B′, C′) observed for NbB_{10}^- are in excellent agreement with the calculated VDEs for the C_{2v} isomer. The lower intensities of these features suggest that the C_{2v} isomer is energetically less stable than the wheel-type structure, again confirming that the global minimum of NbB_{10}^- is also the D_{10h} molecular wheel.

According to the design principle that we proposed recently for stable $M©B_n^{k-}$-type molecular wheels,[18] the valence of the central metal atom should be one for a B_{10} ring. However, both Ta and Nb are known to have five valence electrons. To understand the bonding in the $M©B_{10}^-$ molecular wheels, we present results of the Adaptive Natural Density Partitioning (AdNDP) analysis (see the Experimental Section) for $Ta©B_{10}^-$ in Figure 3. The advantage of the AdNDP analysis is the ability to recover simultaneously both localized and delocalized bonding in chemical species.

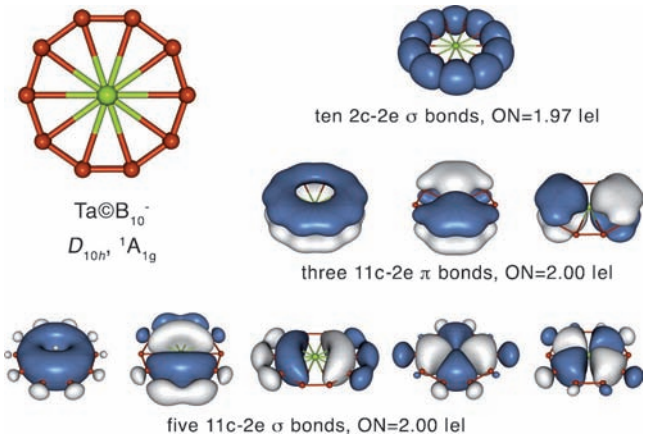

Figure 3. Chemical bonding pattern of $Ta©B_{10}^-$ shown by the AdNDP analysis. ON stands for occupation number.

The AdNDP analysis revealed ten 2c-2e peripheral σ bonds, five delocalized σ bonds (satisfying the $4N+2$ rule for aromaticity with $N=2$), and three delocalized π bonds (satisfying the $4N+2$ rule for aromaticity with $N=1$). A similar bonding pattern was found for $Nb©B_{10}^-$. Thus, both clusters are doubly σ and π aromatic and satisfy the construction model. However, in contrast to the molecular wheels of B_8^{2-}, B_9^-, and $Ru©B_9^-$, there are 10 delocalized σ electrons for the current $M©B_{10}^-$ molecular wheels owing to the strong bonding between the 4d/5d orbitals of Nb/Ta with the peripheral B_{10} ring. Therefore, in these cases, the electronic design principle needs to be revised as $x=16-n-k$ to account for the 10 delocalized σ electrons. This result suggests that more delocalized bonding electrons are required, either in the σ or π framework, to build ever highly coordinated planar molecular wheels.

The two delocalized σ bonds involving the Ta 5d orbitals can be alternatively shown by the AdNDP analysis with low threshold values as d_{xy} and $d_{x^2-y^2}$ lone pairs on the Ta atom with low occupation number (ON) of 1.11 |e| (compared to the ideal value of 2.00 |e|) and therefore the estimated contribution of the Ta 5d atomic orbitals (AOs) to the delocalized bonding is 55%. On the contrary, the molecular wheel structure of the above-mentioned $Au©B_{10}^-$ anion is not the global minimum because the Au 5d AOs remain atom-like and do not participate in delocalized bonding. The availability of d AOs in Nb and Ta for participation in the σ-delocalized bonding with the peripheral ring leads to substantial stabilization of the decagonal doubly aromatic structures of $Nb©B_{10}^-$ and $Ta©B_{10}^-$ and makes them the global minimum structures. Thus, it is conceivable that other early 4d or 5d elements will be able to form not only decagonal $M©B_{10}^{k-}$-type species, but also species with even higher coordination numbers.

Experimental Section

Photoelectron spectroscopy: The experiment was performed using a magnetic bottle photoelectron spectroscopy apparatus equipped with a laser vaporization cluster source that was described in detail previously.[23] Briefly, the transition metal (M)-doped boron clusters were produced by laser ablation (532 nm) of a disk target made of isotopically enriched ^{11}B (around 10%), M (around 10–15%), balanced by Bi or Ag which acted as target binders and also provided calibrants (Bi^- and Ag^-) for the photoelectron spectra. The clusters were entrained by a He carrier gas seeded with 5% Ar and underwent a supersonic expansion to form a collimated and cold molecular beam. The composition and the cooling of the clusters were controlled by the time delay between the carrier gas pulse and the ablation laser. The negatively charged clusters were extracted and analyzed with a time-of-flight mass spectrometer. The species of interest were mass-selected and decelerated before being photodetached by pulsed laser beams at 193 nm (6.424 eV) or 266 nm (4.661 eV). Photoelectrons were collected at nearly 100% efficiency by a magnetic bottle and analyzed in a 3.5 m long electron flight tube. The resolution of the apparatus, $\Delta E/E$, was better than 2.5%, that is, 25 meV for 1 eV electron.

Theoretical calculations: The search for the global minimum structures of the TaB_{10}^- and NbB_{10}^- species was performed using the Coalescence Kick program, written by Averkiev.[7] These calculations were performed at the PBE0/LANL2DZ[24–26] level of theory. The lowest energy isomers ($\Delta E < 50$ kcal mol^{-1}) were then reoptimized at PBE0/Ta, Nb/Stuttgart/B/aug-cc-pVTZ[27–31] (see Figures S1 and S2 in the Supporting Information) and single-point calculations for the four lowest isomers were performed using the RCCSD(T)/Ta, Nb/Stuttgart/B/aug-cc-pVTZ level of theory.

Theoretical VDEs were calculated at the PBE0/Ta, Nb/Stuttgart/B/aug-cc-pVTZ and ROCCSD(T)/Ta, Nb/Stuttgart/B/aug-cc-pVTZ//PBE0/Ta, Nb/Stuttgart/B/aug-cc-pVTZ levels of theory. To explain the around 0.2 eV experimental splitting in the first two peaks of the TaB_{10}^- photoelectron spectrum we performed zero-order relativistic approximation (ZORA) calculations[32,33] with PBE0/QZ4P and M06-2X/QZ4P[34,35] exchange correlation potentials using the ADF program.[36] Results presented in Tables S1 and S2 in the Supporting Information show spin–orbit splitting of around 0.2 eV for both peaks, in an excellent agreement with the experimental observation. Chemical bonding analyses (PBE0/LANL2DZ) of both clusters were performed using the AdNDP method and the AdNDP program written by Zubarev.[37] All non-relativistic calculations were done using Gaussian 09.[38] Molekel 5.4.0.8 was used for MO visualization.[39]

Received: November 9, 2011
Revised: December 30, 2011
Published online: January 20, 2012

Keywords: ab initio calculations · aromaticity · coordination modes · hypercoordination · photoelectron spectroscopy

[1] H. J. Zhai, A. N. Alexandrova, K. A. Birch, A. I. Boldyrev, L. S. Wang, *Angew. Chem.* **2003**, *115*, 6186–6190; *Angew. Chem. Int. Ed.* **2003**, *42*, 6004–6008.
[2] H. J. Zhai, B. Kiran, J. Li, L. S. Wang, *Nat. Mater.* **2003**, *2*, 827–833.
[3] A. N. Alexandrova, H. J. Zhai, L. S. Wang, A. I. Boldyrev, *Inorg. Chem.* **2004**, *43*, 3552–3554.
[4] A. N. Alexandrova, A. I. Boldyrev, H. J. Zhai, L. S. Wang, *Coord. Chem. Rev.* **2006**, *250*, 2811–2866.
[5] D. Yu. Zubarev, A. I. Boldyrev, *J. Comput. Chem.* **2007**, *28*, 251–268.
[6] W. Huang, A. P. Sergeeva, H. J. Zhai, B. B. Averkiev, L. S. Wang, A. I. Boldyrev, *Nat. Chem.* **2010**, *2*, 202–206.
[7] A. P. Sergeeva, B. B. Averkiev, H. J. Zhai, A. I. Boldyrev, L. S. Wang, *J. Chem. Phys.* **2011**, *134*, 224304.
[8] K. Exner, P. v. R. Schleyer, *Science* **2000**, *290*, 1937–1940.

[9] Z.-X. Wang, P. v. R. Schleyer, *Science* **2001**, *292*, 2465 – 2469.
[10] L. M. Wang, W. Huang, B. B. Averkiev, A. I. Boldyrev, L. S. Wang, *Angew. Chem.* **2007**, *119*, 4634 – 4637; *Angew. Chem. Int. Ed.* **2007**, *46*, 4550 – 4553.
[11] B. B. Averkiev, D. Y. Zubarev, L. M. Wang, W. Huang, L. S. Wang, A. I. Boldyrev, *J. Am. Chem. Soc.* **2008**, *130*, 9248 – 9250.
[12] R. Islas, T. Heine, K. Ito, P. v. R. Schleyer, G. Merino, *J. Am. Chem. Soc.* **2007**, *129*, 14767 – 14774.
[13] B. B. Averkiev, A. I. Boldyrev, *Russ. J. Gen. Chem.* **2008**, *78*, 769 – 773.
[14] J. C. Guo, W. Z. Yao, Z. Li, S. D. Li, *Sci. China Ser. B* **2009**, *52*, 566 – 570.
[15] C. Romanescu, A. P. Sergeeva, W. L. Li, A. I. Boldyrev, L. S. Wang, *J. Am. Chem. Soc.* **2011**, *133*, 8646 – 8653.
[16] T. R. Galeev, C. Romanescu, W. L. Li, L. S. Wang, A. I. Boldyrev, *J. Chem. Phys.* **2011**, *135*, 104301.
[17] W. L. Li, C. Romanescu, T. R. Galeev, L. S. Wang, A. I. Boldyrev, *J. Phys. Chem. A* **2011**, *115*, 10391 – 10397.
[18] C. Romanescu, T. R. Galeev, W. L. Li, A. I. Boldyrev, L. S. Wang, *Angew. Chem.* **2011**, *123*, 9506 – 9509; *Angew. Chem. Int. Ed.* **2011**, *50*, 9334 – 9337.
[19] B. B. Averkiev, L. M. Wang, W. Huang, L. S. Wang, A. I. Boldyrev, *Phys. Chem. Chem. Phys.* **2009**, *11*, 9840 – 9849.
[20] C. Q. Miao, J. C. Guo, S. D. Li, *Sci. China Ser. B* **2009**, *52*, 900 – 904.
[21] Z. Pu, K. Ito, P. v. R. Schleyer, Q. S. Li, *Inorg. Chem.* **2009**, *48*, 10679 – 10686.
[22] H. J. Zhai, C. Q. Miao, S. D. Li, L. S. Wang, *J. Phys. Chem. A* **2010**, *114*, 12155 – 12161.
[23] L. S. Wang, H. S. Cheng, J. Fan, *J. Chem. Phys.* **1995**, *102*, 9480 – 9493.
[24] C. Adamo, V. Barone, *J. Chem. Phys.* **1999**, *110*, 6158.
[25] J. P. Perdew, K. Burke, M. Ernzerhof, *Phys. Rev. Lett.* **1996**, *77*, 3865 – 3868.
[26] P. J. Hay, W. R. Wadt, *J. Chem. Phys.* **1985**, *82*, 270.
[27] R. A. Kendall, T. H. Dunning, Jr., R. J. Harrison, *J. Chem. Phys.* **1992**, *96*, 6796.
[28] T. H. Dunning, Jr., *J. Chem. Phys.* **1989**, *90*, 1007.
[29] A. Bergner, M. Dolg, W. Kuechle, H. Stoll, H. Preuss, *Mol. Phys.* **1993**, *80*, 1431 – 1441.
[30] M. Kaupp, P. v. R. Schleyer, H. Stoll, H. Preuss, *J. Chem. Phys.* **1991**, *94*, 1360.
[31] M. Dolg, H. Stoll, H. Preuss, R. M. Pitzer, *J. Phys. Chem.* **1993**, *97*, 5852 – 5859.
[32] C. Chang, M. Pelissier, P. Durand, *Phys. Scr.* **1986**, *34*, 394.
[33] S. Faas, J. G. Snijders, J. H. van Lenthe, E. van Lenthe, E. J. Baerends, *Chem. Phys. Lett.* **1995**, *246*, 632 – 640.
[34] Y. Zhao, D. G. Truhlar, *Theor. Chem. Acc.* **2008**, *120*, 215 – 241.
[35] Y. Zhao, D. G. Truhlar, *Acc. Chem. Res.* **2008**, *41*, 157 – 167.
[36] ADF 2010, SCM, Theoretical Chemistry, Vrije Universiteit, Amsterdam, The Netherlands, http://www.scm.com.
[37] D. Yu. Zubarev, A. I. Boldyrev, *Phys. Chem. Chem. Phys.* **2008**, *10*, 5207 – 5217.
[38] M. J. Frisch et al., GAUSSIAN 09, Rev. B.01, Gaussian, Inc., Wallingford, CT **2009** (see the Supporting Information).
[39] U. Varetto, Molekel 5.4.0.8, Swiss National Supercomputing Centre, Manno, Switzerland, **2009**.

